SCIENTIFIC REP♢RTS

OPEN

Dispersion-Solvent Control of Ionomer Aggregation in a Polymer Electrolyte Membrane Fuel Cell

Ji Hye Lee[1], Gisu Doo[2], Sung Hyun Kwon[1], Sungyu Choi[2], Hee-Tak Kim [2,3] & Seung Geol Lee [1]

In this study, we examined the influence of the dispersion solvent in three dipropylene-glycol/water (DPG/water) mixtures, with DPG contents of 0, 50, and 100 wt%, on ionomer morphology and distribution, using dynamic light scattering (DLS) and molecular-dynamics (MD) simulation techniques. The DLS results reveal that Nafion-ionomer aggregation increases with decreasing DPG content of the solvent. Increasing the proportion of water in the solvent also led to a gradual decrease in the radius of gyration (R_g) of the Nafion ionomer due to its strong backbone hydrophobicity. Correspondingly, MD simulations predict Nafion-ionomer solvation energies of -147 ± 9 kcal/mol in water, -216 ± 21 kcal/mol in the DPG/water mixture, and -444 ± 9 kcal/mol in DPG. These results suggest that higher water contents in mixed DPG/water solvents result in increased Nafion-ionomer aggregation and the subsequent deterioration of its uniform dispersion in the solvent. Moreover, radial distribution functions (RDFs) reveal that the ($-CF_2CF_2-$) backbones of the Nafion ionomer are primarily enclosed by DPG molecules, whereas the sulfonate groups (SO_3^-) of its side chains mostly interact with water molecules.

Polymer electrolyte membrane fuel cells (PEMFCs) are promising renewable energy sources for automobiles, stationary power generators, and portable devices due to their high energy densities, zero emissions, and fast start-up times, at even low operating temperatures[1–5]. However, there still remain several hurdles that need to be overcome before the large-scale commercialization of PEMFCs for electric vehicles can be realized. Further effort research is required in order to reduce the cost of Pt and Pt-alloy catalysts and to improve their durabilities, while optimizing and enhancing their performance. At the heart of a PEMFC is the membrane electrode assembly (MEA), which includes a polymer electrolyte membrane (PEM), or ionomer membrane, which is sandwiched between two anode- and cathode-catalyst layers. In particular, the catalyst layers (CLs) have very thin three-phase boundaries where the electrochemical reactions take place. Each CL consists of an electron-conductive catalyst phase, an ion-conductive polymer-electrolyte phase, and a porous reactant-transport phase. Consequently, CLs are particularly sensitive and demanding, and further studies into their characteristic morphologies are required in order to improve our understanding of them. Conventional CLs are commonly fabricated from catalyst ink dispersions, which are prepared by mixing a carbon supported platinum catalyst (Pt/C), an ionomer, and the dispersion solvent. The catalyst-layer ink is deposited on a diffusion medium or an electrolyte membrane using a number of deposition methods that include decal transfer, spray coating, die coating, screen printing, and inkjet printing. Molecular interactions between the ionomer and the dispersion solvent control the conformations of the ionomer molecules, which subsequently determine the sizes and distributions of the ionomer aggregates in the dispersion solvent; they also govern CL-ink properties, including viscosity, boiling point, rate of solidification, and ultimately the physical and mass-transport properties of the catalyst layer. Therefore, the selection of an appropriate dispersion solvent, and an understanding of the microstructure of the catalyst ink, is vitally important in order to enhance the final performance of the PEMFC.

Much research has focused on the properties of CL inks and the morphologies of the ionomers in CL inks that contain several dispersion solvents. Pioneering work on the effect of the dispersion solvent on the state of Nafion

[1]Department of Organic Material Science and Engineering, Pusan National University, 2, Busandaehak-ro 63beon gil, Geumjeong-gu, Busan, 46241, Republic of Korea. [2]Department of Chemical and Biomolecular Engineering, Korea Advanced Institute of Science and Technology (KAIST), 291 Daehak-ro, Yuseong-gu, Daejeon, 34141, Republic of Korea. [3]Advanced Battery Center, KAIST Institute for the NanoCentury, Korea Advanced Institute of Science and Technology (KAIST), Daejeon, 34141, Republic of Korea. Correspondence and requests for materials should be addressed to H.-T.K. (email: heetak.kim@kaist.ac.kr) or S.G.L. (email: seunggeol.lee@pusan.ac.kr)
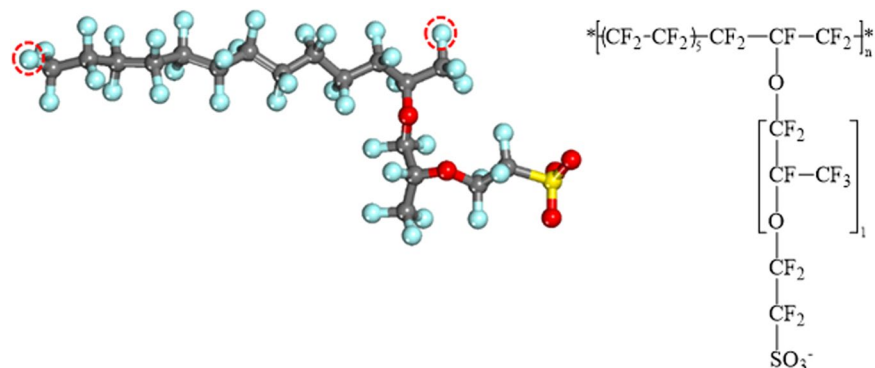
Figure 1. The equilibrated structure (left) and chemical formula (right) of the Nafion monomer. The circles indicate the head and tail atoms in the Nafion-ionomer repeat unit. Carbon, oxygen, fluorine, and sulfur atoms are depicted as gray, red, cyan, and yellow balls, respectively.

ionomers in solution was presented by Uchida *et al.*[6,7] and Shin *et al.*[8], who found that, depending on the dielectric constant (ε) of the solvent, perfluorosulfonate ionomers (PFSIs) can form solutions ($\varepsilon > 10$), colloids ($3 \le \varepsilon \le 10$), or precipitates ($\varepsilon < 3$). Fernandez *et al.*[9] reported the influence of solvent composition and evaporation rate on the microstructure of the catalyst layer and concluded that the dielectric constant of the solvent is a key parameter that needs to be controlled during the preparation of CL inks, which was shown to be directly related to electrode performance. Furthermore, studies on the effect of the dispersion solvent, including methanol, ethanol, 1-propanol, 2-propanol, ethylene glycol, propylene glycol, 1,4-butanediol, glycerol, and their mixtures, among others, on ionomer structure have been conducted using ^{19}F nuclear magnetic resonance (^{19}F NMR) spectroscopy[10-14], cryogenic scanning electron microscopy (cryo-SEM)[15], dynamic light scattering (DLS)[14,16-19], small angle X-ray scattering (SAXS), small angle neutron scattering (SANS)[13,14,19-38], and electron spin resonance (ESR) techniques[11,12], among others[9,39-47]. However, none of these experiments clearly identified ionomer morphologies in CL inks owing to limitation associated with observation scale and the complex inner structures of the CL inks.

Since the design of the ionomer-dispersion solvent is based on the observation that the structures of the Nafion-ionomer aggregates in the CL slurry are highly dependent on the interactions between the dispersion solvent and the ionomers, herein, we conducted a systematic experimental investigation into ionomer microstructure and distribution using the DLS technique and molecular-dynamics (MD) simulations. In this study, we introduce a new ionomer dispersion based on a binary mixture of dipropylene glycol (DPG) and water; this mixture allows the ionomer distribution to be tuned, which affects the power performance of the CL. DPG has a high solvating power for perfluorinated sulfonic acids (PFSAs) and forms nanodispersions of ionomers. Hence, we prepared three types of dispersion solvent, namely water, dipropylene glycol (DPG), and a 1:1 (w/w) DPG/water mixture, and investigated the molecular interactions between the ionomers and the given dispersion solvent as the ionomer-morphology of the solution changed. Upon equilibration of the three types of bulk system, the structural properties of the ionomer in each solvent, which include its radius of gyration (R_g) and radial distribution function (RDF), as well as the solvation energy of the dispersion solvent, were analyzed from a molecular perspective.

Experimental Section

Nafion ionomer aggregation.
We used the dynamic light scattering (DLS) technique to quantify the scale of Nafion-ionomer aggregation in each solvent system. Firstly, Nafion powder, which was obtained from a commercial Nafion D520 solution (DuPont, ion-exchange capacity = 1.00 meq/g), was dispersed in DPG (Sigma-Aldrich)/DI-water mixtures (DPG proportions of 100%, 50%, and 0%) by ball milling and subsequent stirring. Size analysis was performed at 25 °C using DLS equipment (Zetasizer nano ZS90, Malvern Co.). In order to ensure that the influence of Nafion on solvent viscosity was negligible, dispersions were diluted to 1 wt% for precise DLS measurements.

Molecular dynamics simulations.
Model construction. The chemical structure of Nafion ionomer with an equivalent weight (EW) of about 1000 g of dry polymer per mol of sulfonic-acid groups was used as the model of ionomer. The chemical formula and structure of the Nafion ionomer employed in this study are illustrated in Fig. 1. The monomeric unit of the Nafion ionomer consists of a backbone of CF_x groups and a side chain with two ether linkages terminated by a sulfonic acid group; ten repeat units form the Nafion polymer chain. All sulfonic acid groups in the Nafion ionomer were assumed to be fully ionized (in their sulfonate forms) on the basis of experimental infrared-spectroscopic evidence[48,49]. A number of hydronium ions equal to the total number of sulfonate groups in the Nafion ionomer were added in order to ensure charge neutrality.

Water, DPG, and a 1:1 (w/w) DPG/water mixture were selected as the three solvents for this study. Typically, the composition of a CL ink is controlled on the basis of the weight percentage of each component. The weight ratio of the Nafion ionomer to the dispersion solvent was fixed at 1:4 in this study. We selected the 1:4 ratio of ionomer to solvent in the model due to the limitations on the computational resources and costs. The previous research[50] reported that the 1:4 (80 wt% solvent content) ratio can be considered as high solvent content to dominate the overall properties of the system by solvents. Thus, the 1:4 ratio of ionomer to solvent may be a

	Solvent type		
	DPG	DPG/water	water
Simulated cell size (Å)	41.82 ± 0.07	41.36 ± 0.65	42.01 ± 0.06
Number of water molecules	0	1098	2207
Number of DPG molecules	303	149	0

Table 1. MD simulation details.

good indicator for observing the overall inner-structure of ionomer/solvent system to describe the solvent effects at the atomic scale. Mixtures of the Nafion ionomer and each dispersion solvent were randomly packed into three-dimensional cubic boxes using a Monte Carlo (MC) simulation code. Periodic boundary conditions were applied in all three directions. Simulation details for the three ionomer-dispersed solvent systems are summarized at Table 1.

Force Field. The DREIDING force field[51] was employed in this study to describe intermolecular and intramolecular interactions; this force field has been previously used in other fuel-cell studies and various molecular systems[50,52–54]. The F3C[55] and OPLS-AA[56] force fields were used for the water and DPG molecules, respectively. The form of the force field is given by:

$$E_{total} = E_{vdW} + E_{electrostatic} + E_{bond} + E_{angle} + E_{torsion} + E_{inversion}, \tag{1}$$

where E_{total}, E_{vdW}, $E_{electrostatic}$, E_{bond}, $E_{torsion}$, and $E_{inversion}$ are the total energy, and the van der Waals, electrostatic, bond-stretching, angle-bending, torsion, and inversion component energies, respectively. The individual atomic charges were assigned on the basis of quantum-mechanical Mulliken population analyses at the DNP level, using the generalized gradient approximation (GGA) of the Perdew-Burke-Ernzerhof (PBE) functional[57]. The atomic charges on the water molecules were assigned on the basis of the F3C water model. The Particle-Particle Particle-Mesh (PPPM) method[58] was used to calculate electrostatic interactions.

Simulation details. All molecular dynamics (MD) simulations were carried out using the large-scale atomic/molecular massively parallel simulator (LAMMPS) MD code[59]. The equations of motion were integrated using a velocity Verlet algorithm[60] with a time step of 1.0 fs. A damping relaxation time of 0.1 ps and a dimensionless cell mass factor of 1.0 were employed in the Nose-Hoover temperature thermostat[61,62] for the canonical (NVT) and isothermal-isobaric (NPT) ensemble MD simulations. All initial models were first relaxed to their local energy minima using the steepest-descent (SD) and conjugate-gradients (CG) optimization algorithms. Following optimization, a 5 ns NVT MD simulation and a subsequent 15 ns NPT MD simulation were performed at 298.15 K in order to fully equilibrate the structure, from which the last 10 ns of each NPT simulation were used for data collection.

Results and Discussion

Dynamic light scattering.
DLS measurements provided a quantitative comparison of the sizes of the ionomer aggregates in the three solvents, namely water (0% DPG), DPG/water (50% DPG), and DPG (100% DPG). The intensity-distribution plot displayed in Fig. 2 clearly reveals that the ionomer-aggregate size strongly depends on the solvent composition. Because the intensity is proportional to the sixth power of the particle diameter, ionomer aggregates that dominate in the catalyst layer in terms of number or volume must be the small particles in the intensity distribution and below analysis was done with the peak at the smaller diameter. The nanoscale hydrodynamic radius (R_H) of 8 nm determined for 100% DPG reflects the high Nafion-solvating power of DPG. In contrast, pure water (0% DPG) resulted in a micro-scale dispersion ($R_H \sim 1 \mu m$) consistent with severe Nafion-ionomer aggregation resulting from poor interactions between water and the hydrophobic Nafion backbone. A submicron-scale Nafion dispersion ($R_H \sim 50$ nm) was obtained at an intermediate DPG/water composition (50% DPG), due to a combination of interactions between the Nafion ionomer and both the DPG and water. It should be noted that the DLS assumes the aggregates as perfect spheres, which is not true, therefore accurate size or shape of the Nafion ionomer aggregate are not available from DLS data. Nonetheless, it was sufficient to investigate the molecular interactions from the different size scales from tens of nm to micron for the solvents.

Equilibrated structure.
To explain these experimental observations, a theoretical model was developed in order to acquire detailed atomic-scale Nafion-ionomer-chain information, and to predict the distribution of the Nafion ionomer within the catalyst ink. The dispersion solvent plays a key role in determining ionomer morphology and distribution in this MD study. Final snapshots of the equilibrated structures in the three dispersion solvents, starting from randomly dispersed ionomer structures, are depicted in Fig. 3a–c. As illustrated in Fig. 3, the backbone (-CF$_2$CF$_2$-) components of the Nafion ionomer tend to aggregate together in water due to the hydrophobic nature of the backbone, which is unwilling to interact with water; the Nafion-ionomer backbone chains form hydrophobic core regions in the aggregated structures. At the same time, the side chains and their sulfonate (SO$_3^-$) groups protrude from this core region into the dispersion-solvent medium, which is ascribable to their high affinities for water molecules because of their hydrophilic and ionic properties. On the contrary, the majority of the (-CF$_2$CF$_2$-) backbones of the Nafion appear to be extended and remain in a dispersed (or non-localized) state in DPG, which is due to favorable hydrophobic interactions between the backbones of the Nafion ionomer and the DPG solvent. Furthermore, the relatively strong hydrophobicity of the DPG molecule, compared to water,
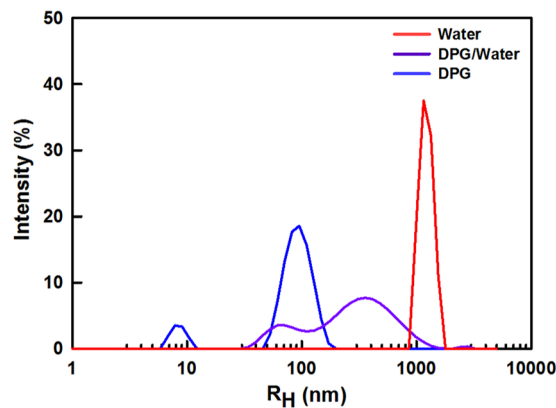
3

Figure 2. R_H intensity distributions for the Nafion-ionomer aggregates in 100% DPG, 50% DPG, and 0% DPG solvents as determined by DLS measurements.
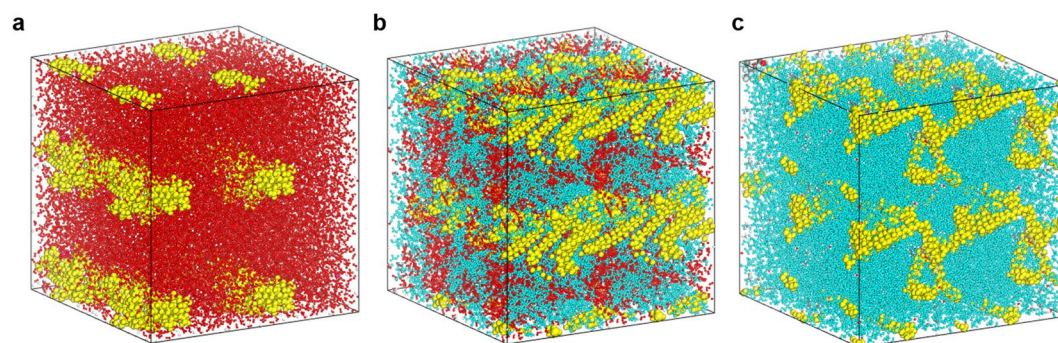

Figure 3. Nafion-ionomer equilibrium structures in $2 \times 2 \times 2$ supercells in (**a**) water, (**b**) 1:1 (w/w) DPG/water, and (**c**) DPG. The Nafion ionomer, DPG, and water molecules are depicted in yellow, cyan, and red, respectively.

results in the localization of the hydrophilic sulfonic sulfonate groups (SO_3^-) of the Nafion ionomer. The equilibrated structure of the Nafion ionomer did not appear to adopt any special backbone or side-chain aggregation in the mixed DPG/water solvent. Detailed analysis of the Nafion ionomer microstructure in the DPG/water mixture was facilitated by radial distribution function (RDF) calculations. The RDF ($g_{A-B}(r)$) is a density function that describes the probability of finding atoms A and B at a distance r averaged over the equilibrium trajectory. This function reflects the characteristics of the microstructure; it can be used to reveal the essence of the interactions that occur between non-bonding atoms and can be applied to the structural investigations of solids and liquids. The RDF is calculated by:

$$g_{A-B}(r) = \left(\frac{n_B}{4\pi r^2 dr} \right) / \left(\frac{N_B}{V} \right),$$

(2)

where n_B is the number of B particles located at a distance r in a shell of thickness dr from particle A, N_B is the number of B particles in the system, and V is the total volume of the system. Using this function, it is possible to determine the environment that the guest molecules are in. In order to directly compare intensities, the products of the pair correlations and number densities ($\rho g_{A-B}(r)$) are used instead of $g_{A-B}(r)$. Figure 4a displays the RDFs for interactions between the Nafion ionomer and the DPG and water molecules in the mixed DPG/water dispersion solvent. Interestingly, the equilibrated structure of the Nafion ionomer in the DPG/water mixture appears to have the Nafion ionomers mainly surrounded by DPG molecules, as shown in Fig. 4a. In contrast, the water molecules appear to be located on the outsides of the DPG molecules that cover the Nafion ionomers. Figure 4a clearly shows that the first S(Nafion)-O(water) pair peak occurs at a noticeably shorter distance and is more intense than the analogous S(Nafion)-O(DPG) pair peak. This indicates that the regions in the vicinity of the sulfonate groups of the Nafion-ionomer side chain are more populated by water molecules than DPG molecules, which is ascribable to strong electrostatic and hydrophilic interactions between the ionic sulfonate groups of the Nafion ionomer and the polar water molecules. Consequently, the RDF analysis is consistent with the intuitional equilibrium structure.

Radius of gyration. We also calculated ionomer radii of gyration in order to quantitatively analyze the form of the ionomer in the dispersion solvent. The radius of gyration (R_g) of an ionomer is defined as the average-squared distance of any point in the object from its center of mass, according to:
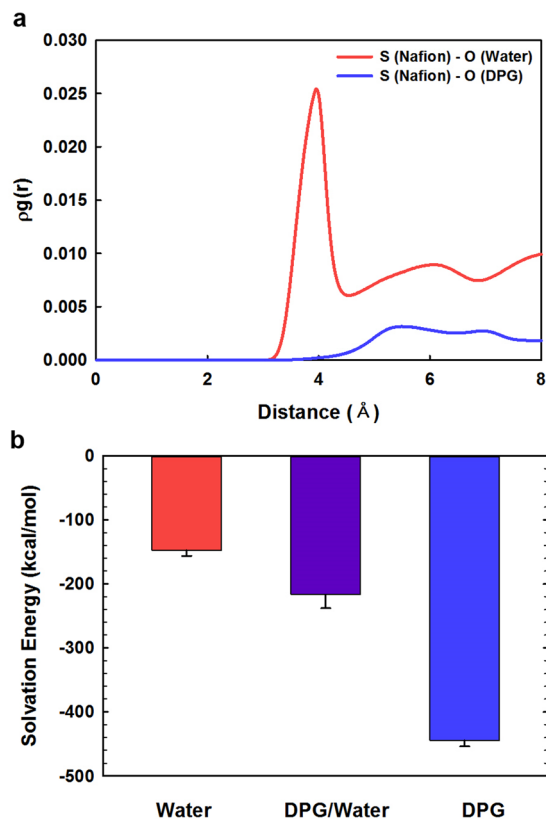
Figure 4. (**a**) RDFs for the Nafion ionomer in the mixed DPG/water dispersion solvent, and (**b**) the solvation energy of the Nafion ionomer in each solvent system.

$$R_g = \left(\frac{1}{N} \sum_{i=1}^{N} (R_i - R_{cm})^2 \right)^{1/2},$$
(3)

where R_i denotes the position vector of the ith atom in the ionomer chain, R_{cm} denotes the position vector of the center of mass of the ionomer chain, and N is the total number of atoms in the ionomer chain at a given time. The R_gs of Nafion-ionomer chains depend largely on the type of dispersion solvent. The R_g of the Nafion ionomer is shorter with increasing weight-fraction of water in the solvent, through aggregation. The average R_g values of the Nafion ionomer in each solvent were determined to be 13.6 ± 0.4 Å in water, 14.7 ± 0.7 Å in 1:1 (w/w) DPG/water, and 17.2 ± 1.0 Å in DPG. These trends are consistent with the visually observable trends depicted in Fig. 3a–c. Obviously R_H and R_g are not the same values to compare the results, however, at the atomic scale, R_g also gives us the valuable information to describe the interaction between the ionomer and the selected solvents. Accordingly, the ionomer chain in water has smaller R_g than DPG, because the hydrophobic main chain (-CF$_2$CF$_2$-) of ionomer tends to aggregate together in water due to the hydrophobic nature of the backbone. Meanwhile, the ionomer relatively well interacts with DPG solvents that leads higher R_g value than that of in water.

Solvation energy. Few previously reported studies have investigated the importance of molecular interactions between ionomers and the dispersion solvent. Kim *et al.*[38] reported that the ability of the solvent to mobilize the Nafion ionomer significantly influences the CL structure. They found that CLs fabricated using solvents with high main-chain mobilities created higher levels of intimate contact at triple-phase boundaries, which were mainly due to strong interactions between solvent molecules and the Nafion ionomers; this, in turn enhances electrochemical performance. Furthermore, the Los Alamos National Laboratory group[13,36,38] investigated the morphologies of Nafion in various solvents by SANS and examined the corresponding electrochemical and mechanical properties. They suggested that fuel-cell-performance durability can be controlled by tuning the properties of the interface between the catalyst and the ionomer through the judicious choice of dispersion medium. Hence, in order to better quantify the interactions between the Nafion ionomer and the dispersion solvent, the solvation energies of the ionomer in the three dispersion solvents were calculated. The solvation energy ($\Delta E_{solvation}$) is used to measure the relative solubility of a polymer in a solvent and is given by:

$$\Delta E_{solvation} = E_{system} - (E_{ionomer} + E_{solvent}),$$
(4)

where E_{system} is the total energy of the ionomer in the solvent, $E_{ionomer}$ is the energy of ionomer, and $E_{solvent}$ is the energy of the solvent. A negative solvation energy indicates good dispersion or solvation of the Nafion ionomer. As shown in Fig. 4b, the solvation energies of the Nafion ionomer are -147 ± 9, -216 ± 21, and -444 ± 9 kcal/mol

in water, 1:1 (w/w) water/DPG, and DPG, respectively. The solvation energy of the Nafion ionomer in DPG is the most negative among the three solvents, which indicates that the Nafion ionomer is well dispersed in DPG. Nafion-ionomer dispersion worsens with increasing levels of water in the solvent, which is in good agreement with the DLS data and the MD results previously discussed.

Conclusions

Herein, we developed a molecular-level understanding of the structure and dynamics of Nafion ionomers in three types of dispersion solvent using DLS and MD techniques. We used three dispersion solvents with different percentages of DPG in water, namely 100, 50, and 0% (w/w). From an experimental perspective, the ionomer-aggregate size increased in the following order: DPG (R_H ~8 nm) < DPG/water (R_H ~50 nm) < water (R_H ~1 μm). Severe Nafion-ionomer aggregation was observed with increasing levels of water in the solvent. Combining the radius-of-gyration (R_g) values of the Nafion ionomers with visual inspections of the equilibrated configurations clearly revealed that increasing water content in the mixed DPG/water solvents resulted in reduced ionomer R_g values that follow the order: water (13.6 ± 0.4 Å) < water/DPG (14.7 ± 0.7 Å) < DPG (17.2 ± 1.0 Å). Likewise, Nafion-ionomer solvation-energy calculations predict that solvation energy increases with increasing water content, and follows the order: (-444 ± 9 kcal/mol) < DPG/water (-216 ± 21 kcal/mol) < water (-147 ± 9 kcal/mol). Among the three solvents, the Nafion ionomer dispersed in DPG exhibited the most negative solvation energy, which indicates that the ionomer retains a well-dispersed state in the DPG system. Meanwhile, Nafion-ionomer aggregation worsened in water. Finally, RDF analyses revealed that the (-CF_2CF_2-) backbones in the Nafion ionomers are predominantly surrounded by DPG molecules, which is ascribable to hydrophobic interactions, whereas the side-chain sulfonate groups (SO_3^-) strongly interact with water molecules due to electrostatic interactions.

References

1. Ticianelli, E. A., Derouin, C. R., Redondo, A. & Srinivasan, S. Methods to Advance Technology of Proton-Exchange Membrane Fuel-Cells. *Journal of the Electrochemical Society* **135**, 2209–2214 (1988).
2. Steele, B. C. H. & Heinzel, A. Materials for fuel-cell technologies. *Nature* **414**, 345–352 (2001).
3. Wang, Y., Chen, K. S., Mishler, J., Cho, S. C. & Adroher, X. C. A review of polymer electrolyte membrane fuel cells: Technology, applications, and needs on fundamental research. *Applied Energy* **88**, 981–1007 (2011).
4. Kraytsberg, A. & Ein-Eli, Y. Review of Advanced Materials for Proton Exchange Membrane Fuel Cells. *Energy & Fuels* **28**, 7303–7330 (2014).
5. Sharaf, O. Z. & Orhan, M. F. An overview of fuel cell technology: Fundamentals and applications. *Renewable & Sustainable Energy Reviews* **32**, 810–853 (2014).
6. Uchida, M., Aoyama, Y., Eda, N. & Ohta, A. New Preparation Method for Polymer-Electrolyte Fuel-Cells. *Journal of the Electrochemical Society* **142**, 463–468 (1995).
7. Uchida, M., Aoyama, Y., Eda, N. & Ohta, A. Investigation of the microstructure in the catalyst layer and effects of both perfluorosulfonate ionomer and PTFE-Loaded carbon on the catalyst layer of polymer electrolyte fuel cells. *Journal of the Electrochemical Society* **142**, 4143–4149 (1995).
8. Shin, S. J. *et al.* Effect of the catalytic ink preparation method on the performance of polymer electrolyte membrane fuel cells. *Journal of Power Sources* **106**, 146–152 (2002).
9. Fernandez, R., Ferreira-Aparicio, P. & Daza, L. PEMFC electrode preparation: Influence of the solvent composition and evaporation rate on the catalytic layer microstructure. *Journal of Power Sources* **151**, 18–24 (2005).
10. Schlick, S., Gebel, G., Pineri, M. & Volino, F. F-19 Nmr-Spectroscopy of Acid Nafion Membranes and Solutions. *Macromolecules* **24**, 3517–3521 (1991).
11. Szajdzinskapietek, E., Schlick, S. & Plonka, A. Self-Assembling of Perfluorinated Polymeric Surfactants in Nonaqueous Solvents - Electron-Spin-Resonance Spectra of Nitroxide Spin Probes in Nafion Solutions and Swollen Membranes. *Langmuir* **10**, 2188–2196 (1994).
12. Szajdzinskapietek, E., Schlick, S. & Plonka, A. Self-Assembling of Perfluorinated Polymeric Surfactants in Water - Electron-Spin-Resonance Spectra of Nitroxide Spin Probes in Nafion Solutions and Swollen Membranes. *Langmuir* **10**, 1101–1109 (1994).
13. Welch, C. *et al.* Nafion in Dilute Solvent Systems: Dispersion or Solution? *Acs Macro Letters* **1**, 1403–1407 (2012).
14. Yamaguchi, M. *et al.* Dispersion of Rod-like Particles of Nafion in Salt-Free Water/1-Propanol and Water/Ethanol Solutions. *Journal of Physical Chemistry B* **118**, 14922–14928 (2014).
15. Takahashi, S., Mashio, T., Horibe, N., Akizuki, K. & Ohma, A. Analysis of the Microstructure Formation Process and Its Influence on the Performance of Polymer Electrolyte Fuel-Cell Catalyst Layers. *Chemelectrochem* **2**, 1560–1567 (2015).
16. Cirkel, P. A., Okada, T. & Kinugasa, S. Equilibrium aggregation in perfluorinated ionomer solutions. *Macromolecules* **32**, 531–533 (1999).
17. Jiang, S. H., Xia, K. Q. & Xu, G. Effect of additives on self-assembling behavior of Nafion in aqueous media. *Macromolecules* **34**, 7783–7788 (2001).
18. Lee, S. J., Yu, T. L., Lin, H. L., Liu, W. H. & Lai, C. L. Solution properties of nafion in methanol/water mixture solvent. *Polymer* **45**, 2853–2862 (2004).
19. Ma, C. H. *et al.* Morphology and properties of Nafion membranes prepared by solution casting. *Polymer* **50**, 1764–1777 (2009).
20. Gierke, T. D., Munn, G. E. & Wilson, F. C. The Morphology in Nafion Perfluorinated Membrane Products, as Determined by Wide-Angle and Small-Angle X-Ray Studies. *Journal of Polymer Science Part B-Polymer Physics* **19**, 1687–1704 (1981).
21. Fujimura, M., Hashimoto, T. & Kawai, H. Small-Angle X-Ray-Scattering Study of Perfluorinated Ionomer Membranes .1. Origin of 2 Scattering Maxima. *Macromolecules* **14**, 1309–1315 (1981).
22. Fujimura, M., Hashimoto, T. & Kawai, H. Small-Angle X-Ray-Scattering Study of Perfluorinated Ionomer Membranes .2. Models for Ionic Scattering Maximum. *Macromolecules* **15**, 136–144 (1982).
23. Kumar, S. & Pineri, M. Interpretation of Small-Angle X-Ray and Neutron-Scattering Data for Perfluorosulfonated Ionomer Membranes. *Journal of Polymer Science Part B-Polymer Physics* **24**, 1767–1782 (1986).
24. Aldebert, P., Dreyfus, B. & Pineri, M. Small-Angle Neutron-Scattering of Perfluorosulfonated Ionomers in Solution. *Macromolecules* **19**, 2651–2653 (1986).
25. Gebel, G., Aldebert, P. & Pineri, M. Structure and Related Properties of Solution-Cast Perfluorosulfonated Ionomer Films. *Macromolecules* **20**, 1425–1428 (1987).
26. Aldebert, P. *et al.* Rod Like Micellar Structures in Perfluorinated Ionomer Solutions. *Journal De Physique* **49**, 2101–2109 (1988).
27. Moore, R. B. & Martin, C. R. Chemical and Morphological Properties of Solution-Cast Perfluorosulfonate Ionomers. *Macromolecules* **21**, 1334–1339 (1988).

28. Moore, R. B. & Martin, C. R. Morphology and Chemical-Properties of the Dow Perfluorosulfonate Ionomers. *Macromolecules* **22**, 3594–3599 (1989).
29. Gebel, G. & Loppinet, B. Colloidal structure of ionomer solutions in polar solvents. *Journal of Molecular Structure* **383**, 43–49 (1996).
30. Loppinet, B., Gebel, G. & Williams, C. E. Small-angle scattering study of perfluorosulfonated ionomer solutions. *Journal of Physical Chemistry B* **101**, 1884–1892 (1997).
31. Gebel, G. & Lambard, J. Small-angle scattering study of water-swollen perfluorinated ionomer membranes. *Macromolecules* **30**, 7914–7920 (1997).
32. Gebel, G. Structural evolution of water swollen perfluorosulfonated ionomers from dry membrane to solution. *Polymer* **41**, 5829–5838 (2000).
33. Rubatat, L., Rollet, A. L., Gebel, G. & Diat, O. Evidence of elongated polymeric aggregates in Nafion. *Macromolecules* **35**, 4050–4055 (2002).
34. Rubatat, L., Gebel, G. & Diat, O. Fibrillar structure of Nafion: Matching Fourier and real space studies of corresponding films and solutions. *Macromolecules* **37**, 7772–7783 (2004).
35. Lin, H. L., Yu, T. L., Huang, C. H. & Lin, T. L. Morphology study of nafion membranes prepared by solutions casting. *Journal of Polymer Science Part B-Polymer Physics* **43**, 3044–3057 (2005).
36. Kim, Y. S. *et al.* Highly durable fuel cell electrodes based on ionomers dispersed in glycerol. *Physical Chemistry Chemical Physics* **16**, 5927–5932 (2014).
37. Shibayama, M. *et al.* SANS Studies on Catalyst Ink of Fuel Cell. *Journal of Applied Polymer Science* **131** (2014).
38. Kim, Y. S. *et al.* Origin of Toughness in Dispersion-Cast Nafion Membranes. *Macromolecules* **48**, 2161–2172 (2015).
39. Kim, J. H., Ha, H. Y., Oh, I. H., Hong, S. A. & Lee, H. I. Influence of the solvent in anode catalyst ink on the performance of a direct methanol fuel cell. *Journal of Power Sources* **135**, 29–35 (2004).
40. Aldebert, P., Gebel, G., Loppinet, B. & Nakamura, N. Polyelectrolyte Effect in Perfluorosulfonated Ionomer Solutions. *Polymer* **36**, 431–434 (1995).
41. Yang, T. H., Yoon, Y. G., Park, G. G., Lee, W. Y. & Kim, C. S. Fabrication of a thin catalyst layer using organic solvents. *Journal of Power Sources* **127**, 230–233 (2004).
42. Chisaka, M. & Daiguji, H. Effect of glycerol on micro/nano structures of catalyst layers in polymer electrolyte membrane fuel cells. *Electrochimica Acta* **51**, 4828–4833 (2006).
43. Chisaka, M., Matsuoka, E. & Daiguji, H. Effect of Organic Solvents on the Pore Structure of Catalyst Layers in Polymer Electrolyte Membrane Fuel Cells. *Journal of the Electrochemical Society* **157**, B1218–B1221 (2010).
44. Therdthianwong, A., Ekdharmasuit, P. & Therdthianwong, S. Fabrication and Performance of Membrane Electrode Assembly Prepared by a Catalyst-Coated Membrane Method: Effect of Solvents Used in a Catalyst Ink Mixture. *Energy & Fuels* **24**, 1191–1196 (2010).
45. Millington, B., Du, S. F. & Pollet, B. G. The effect of materials on proton exchange membrane fuel cell electrode performance. *Journal of Power Sources* **196**, 9013–9017 (2011).
46. Huang, D. C. *et al.* Effect of Dispersion Solvent in Catalyst Ink on Proton Exchange Membrane Fuel Cell Performance. *International Journal of Electrochemical Science* **6**, 2551–2565 (2011).
47. Ngo, T. T., Yu, T. L. O. & Lin, H. L. Nafion-based membrane electrode assemblies prepared from catalyst inks containing alcohol/water solvent mixtures. *Journal of Power Sources* **238**, 1–10 (2013).
48. Laporta, M., Pegoraro, M. & Zanderighi, L. Perfluorosulfonated membrane (Nafion): FT-IR study of the state of water with increasing humidity. *Physical Chemistry Chemical Physics* **1**, 4619–4628 (1999).
49. Gruger, A., Regis, A., Schmatko, T. & Colomban, P. Nanostructure of Nafion (R) membranes at different states of hydration - An IR and Raman study. *Vibrational Spectroscopy* **26**, 215–225 (2001).
50. Lee, S. G., Brunello, G. F., Jang, S. S. & Bucknall, D. G. Molecular dynamics simulation study of P (VP-co-HEMA) hydrogels: Effect of water content on equilibrium structures and mechanical properties. *Biomaterials* **30**, 6130–6141 (2009).
51. Mayo, S. L., Olafson, B. D. & Goddard, W. A. Dreiding - a Generic Force-Field for Molecular Simulations. *Journal of Physical Chemistry* **94**, 8897–8909 (1990).
52. Brunello, G., Lee, S. G., Jang, S. S. & Qi, Y. A molecular dynamics simulation study of hydrated sulfonated poly(ether ether ketone) for application to polymer electrolyte membrane fuel cells: Effect of water content. *J Renew Sustain Ener* **1** (2009).
53. Brunello, G. F. *et al.* Interactions of Pt nanoparticles with molecular components in polymer electrolyte membrane fuel cells: multi-scale modeling approach. *Rsc Adv* **6**, 69670–69676 (2016).
54. Lee, S. G. *et al.* Deswelling Mechanisms of Surface-Grafted Poly(NIPAAm) Brush: Molecular Dynamics Simulation Approach. *Journal of Physical Chemistry C* **116**, 15974–15985 (2012).
55. Levitt, M., Hirshberg, M., Sharon, R., Laidig, K. E. & Daggett, V. Calibration and testing of a water model for simulation of the molecular dynamics of proteins and nucleic acids in solution. *Journal of Physical Chemistry B* **101**, 5051–5061 (1997).
56. Jorgensen, W. L., Maxwell, D. S. & TiradoRives, J. Development and testing of the OPLS all-atom force field on conformational energetics and properties of organic liquids. *J Am Chem Soc* **118**, 11225–11236 (1996).
57. Perdew, J. P., Burke, K. & Wang, Y. Generalized gradient approximation for the exchange-correlation hole of a many-electron system. *Phys Rev B* **54**, 16533–16539 (1996).
58. Hockney, R. W. & Eastwood, J. W. *Computer simulation using particles.* (McGraw-Hill International Book Co., 1981).
59. Plimpton, S. Fast Parallel Algorithms for Short-Range Molecular-Dynamics. *Journal of Computational Physics* **117**, 1–19 (1995).
60. Swope, W. C., Andersen, H. C., Berens, P. H. & Wilson, K. R. A Computer-Simulation Method for the Calculation of Equilibrium-Constants for the Formation of Physical Clusters of Molecules - Application to Small Water Clusters. *Journal of Chemical Physics* **76**, 637–649 (1982).
61. Nose, S. A Unified Formulation of the Constant Temperature Molecular-Dynamics Methods. *Journal of Chemical Physics* **81**, 511–519 (1984).
62. Hoover, W. G. Canonical Dynamics - Equilibrium Phase-Space Distributions. *Physical Review A* **31**, 1695–1697 (1985).

Acknowledgements

Author Contributions

J.H.L. and S.H.K. performed the molecular dynamics simulations. G.D. and S.C. performed the experiments. H.-T.K. and S.G.L. conceived the research idea and wrote the main manuscript text. All authors reviewed the manuscript.

Additional Information

Competing Interests: The authors declare no competing interests.

Publisher's note: Springer Nature remains neutral with regard to jurisdictional claims in published maps and institutional affiliations.